Supporting Information for

Effects of the sample matrix on the photobleaching and photodegradation of toluene-derived secondary organic aerosol compounds

Alexandra L. Klodt[1], Marley Adamek[2], Monica Dibley[2], Sergey A. Nizkorodov[1*], Rachel E. O'Brien[2*]

[1]Department of Chemistry, University of California, Irvine, CA, USA

[2]Department of Chemistry, William & Mary, Williamsburg, VA, USA

Summary of Experiments Conducted

Table S1. Summary of the experiments carried out as part of this study at the College of William and Mary (WM) and the University of California Irvine (UCI).

Experiment Description	**Data sets collected**	**Location**
SOA preparation (x14)	Online-AMS	UCI
Trial experiments on aging of SOA in the aqueous phase (x5)	UV-Vis, LC-ESI-MS	UCI
Trial experiments on aging of SOA on filters (x2)	UV-Vis, Direct infusion ESI-MS, FTIR	WM
Aging of SOA in water and in 1 M ammonium sulfate (x3)	UV-Vis, LC-ESI-MS	UCI
Aging of SOA in water and on filter (x4)	UV-Vis, LC-ESI-MS, offline-AMS	UCI

Aqueous Aging Summary

Table S2. Summary of aqueous SOA samples and their mass concentrations for aqueous-phase photolysis experiments. Mass concentrations from the same filter vary slightly between experiments aged in water versus aged in ammonium sulfate because the exact mass of the filter half was divided by the total mass of the filter and then multiplied by the mass of SOA collected in an attempt to account for differences in sizes of the filter sections. The mass concentrations are still somewhat approximate because the SOA may not have been completely evenly distributed on the filter after collection.

Photolysis experiment	Filter Number	Mass concentration for photolysis (μg mL^{-1})
Water 1	4	233
Water 2	5	220
Water 3	6	238
Ammonium Sulfate 1	4	224
Ammonium Sulfate 2	5	249
Ammonium Sulfate 3	6	253

Scaling Photodegradation Rates to Atmospheric Conditions

The effective rate of photodegradation of SOA is given by

$$J = \int F(\lambda)\phi(\lambda)\sigma(\lambda)d\lambda$$

where $F(\lambda)$ is the surface-area-normalized photon flux, $\phi(\lambda)$ is the quantum yield for dissociation, and $\sigma(\lambda)$ is the base e absorption cross-section of the SOA. To calculate the predicted relative photodegradation rate in the atmosphere, we assumed the dissociation quantum yield was constant over the UV region (280 to 400 nm) and that the absorption cross-section of the SOA could be expressed as the measured mass absorption coefficient (MAC) times a wavelength-independent constant. The relative rate of photodegradation in the atmosphere then simplifies to

$$\frac{J_{atmosphere}}{J_{lamp}} = \frac{\int F_{atmosphere}(\lambda)MAC(\lambda)d\lambda}{\int F_{lamp}(\lambda)MAC(\lambda)d\lambda}.$$

The surface-area-normalized photon flux ($F(\lambda)$) and the surface-area-normalized photon flux convoluted with MAC ($F(\lambda) \times MAC(\lambda)$) for our photolysis set-up, the 24 h average values for LA (taken on June 20th), and the maximal achievable flux at the SZA = 0 are shown in Figure S1, and the ratios of theoretical atmospheric photodegradation rate to photodegradation rate in our set-up is shown in Table S3. The parameters used for the “Quick TUV” calculator (ACOM: Quick TUV, 2019) which was used to estimate the spectral flux densities were:

- Latitude/Longitude: 34°N 118°W or SZA = 0
- Date and Time: June 20, 2021
- Overhead Ozone: 300 du
- Surface Albedo: 0.1
- Ground Altitude: 0 km
- Measured Altitude: 0 km
- Clouds Optical Depth/Base/Top: 0.00/4.00/5.00
- Aerosols Optical Depth/S-S Albedo/Alpha: 0.235/0.990/1.000
- Sunlight Direct Beam/Diffuse Down/Diffuse Up: 1.0/1.0/0.0
- 4 streams transfer model.

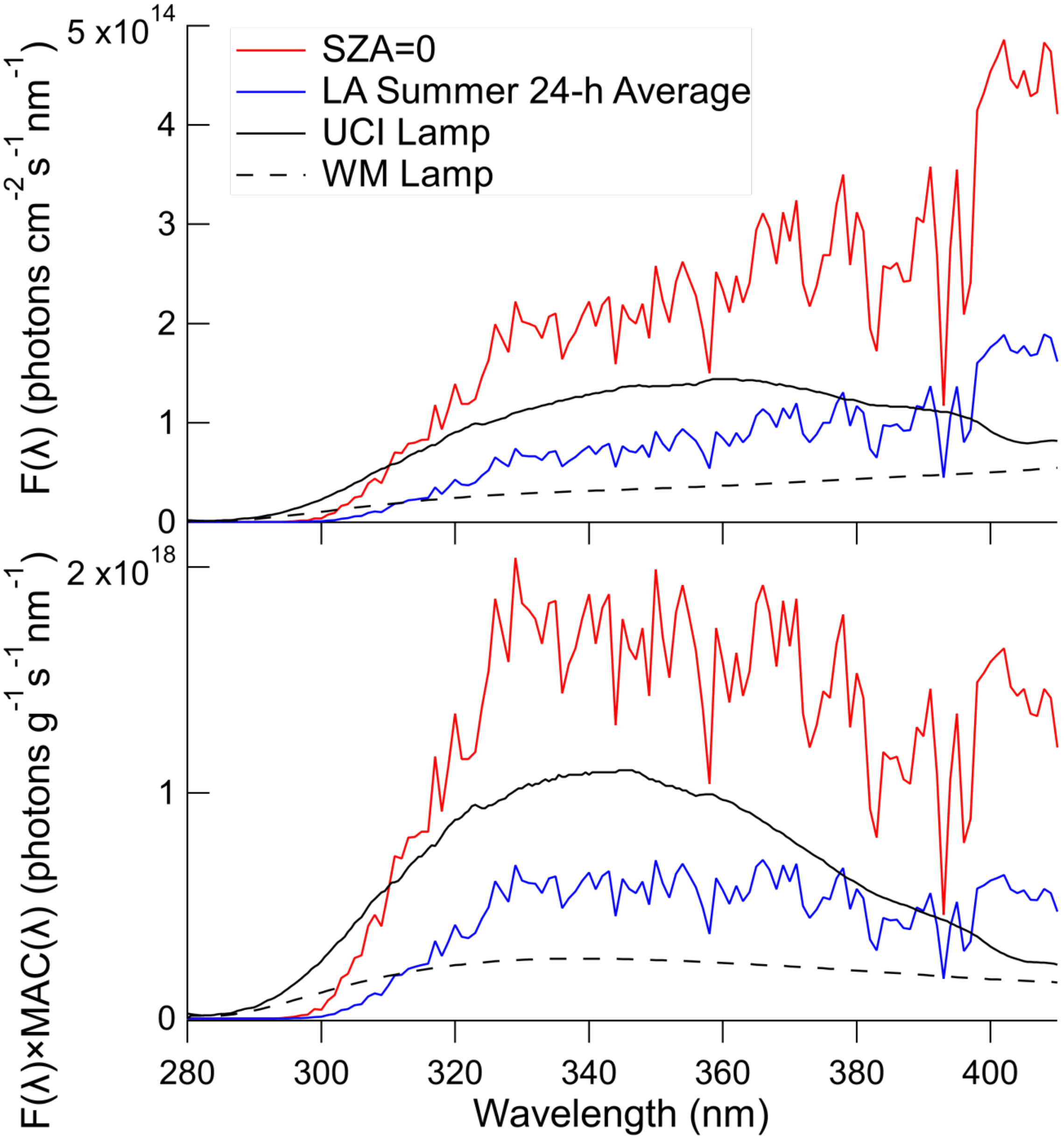

Figure S1. Spectral flux density ($F(\lambda)$) the convolution of spectral flux density and mass absorption coefficient ($F(\lambda) \times MAC(\lambda)$) comparison for UCI photolysis lamp (black), solar zenith angle zero (red), and the Los Angeles 24-h average (blue).

Table S3. The integrated fluxes and the number of hours equivalent to one hour under our photolysis set-up for the 24-h average solar flux in Los Angeles in summer and the maximal achievable flux at the SZA = 0. The calculation was performed by integrating $F(\lambda) \times MAC(\lambda)$ from Figure S2 from 280 to 400 nm, the UV wavelength range that likely drives photochemistry for our samples. The values on the last two columns represent the ratios of the UV lamp's integrated flux to the solar integrated flux.

Location	**Integrated $F(\lambda) \times MAC(\lambda)$ from the UV lamp (photons g^{-1} s^{-1})**	**Integrated $F(\lambda) \times MAC(\lambda)$ at SZA=0 (photons g^{-1} s^{-1})**	**Integrated $F(\lambda) \times MAC(\lambda)$ from the 24-h average in Los Angeles (photons g^{-1} s^{-1})**	**Equivalent hours at SZA=0**	**Equivalent hours at 24-h average sunlight in LA**
UCI	7.94E19	1.32E20	4.62E19	0.6	1.7
WM	2.35E19	1.32E20	4.62E19	0.2	0.5

Extraction Efficiency Determination

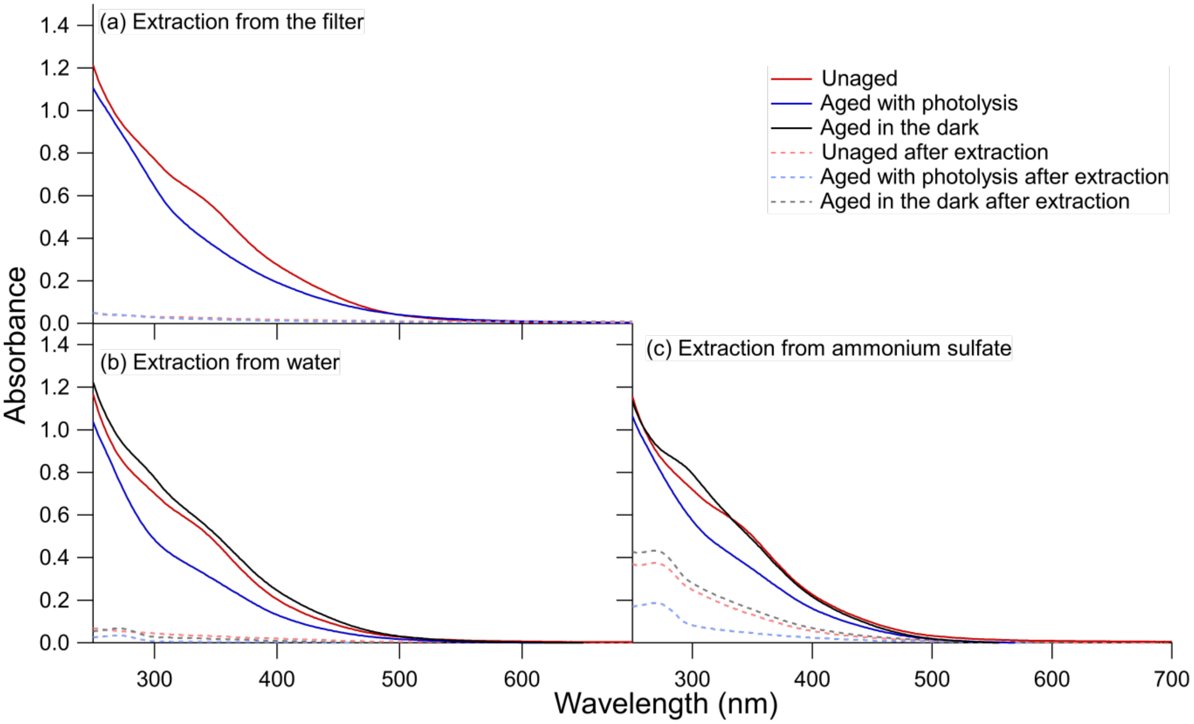

Figure S2. A test of the extraction efficiency of the toluene BrC SOA (a) from the Teflon filters, (b) from the pure water solutions, and (c) from the 1 M ammonium sulfate solutions. After filters were initially extracted in acetonitrile, the filters were then submerged in 3 mL of methanol and shaken (but not stirred) for 10 minutes to extract any remaining SOA. Assuming that the integrated absorbance between 250 nm and 550 nm can be used as a metric for the amount of extracted SOA, >90% of the SOA was extracted from the filters. Recovery efficiency from the water and ammonium sulfate experiments was determined by adding 1 mL of water back to vial the SOA was extracted from, replacing the 1 mL of water which had been removed by rotary evaporation after SOA was extracted as described in the main text. Panel (b) shows that >90% of the SOA was recovered in the pure water conditions, but only 50 to 70% of the SOA could be recovered from the ammonium sulfate conditions in panel (c).

Methods for preliminary experiments at WM

WM Sample Preparation and Irradiation

The first set of on-filter photolysis experiments were carried out at the WM. Samples were irradiated in a photolysis box that has been described previously (Walhout et al., 2019). Briefly, the filter was sliced into four segments and three of the segments were placed in the box mounted vertically in front of a Xenon arc lamp (Newport model 66902). The photolysis box was air-tight, had a Teflon film (0.001 in inch) taped across a hole cut into the front panel to allow the UV radiation pass through, and had ~1-2 L min^{-1} of zero air (Environics 7000) at 50-60% RH continuously flowing through it. The spectral flux density on the irradiated filters is shown in Fig. S1. A second dark box was placed after the photolysis box with the same air flow. The control filter segment was placed there immediately, the second filter segment was moved there after 6 h of photolysis, the third filter segment was moved there after 18 h, and the irradiation ended after 24 h. This ensured that all the filter segments were exposed to the same air flow for the same amount of time, resulting in comparable SOA material loss to vaporization. The observed differences should therefore be dominantly due to photolysis, although we cannot fully rule out additional volatilization due to absorption of light by the chromophores in the SOA material.

WM ATR-FTIR

A Shimadzu IR Tracer-100 MIRacle 10 with a diamond crystal ATR probe was used to collect ATR-FTIR spectra from 600-4000 cm^{-1}. A total of 45 scans were averaged per sample, and for each sample, an air background was collected before the filter was adhered to the crystal. After irradiating the filter segments for 0 (control), 6, 18 and 24 h, small slivers of the filters were cut off and pressed onto an ATR-FTIR crystal (diamond) using the swivel press. The filters were then detached, an unpressed area of the filter was moved overtop the crystal and the filter was pressed onto the crystal again. After the second press, the filters were removed from the crystal, leaving behind a thin film of sample material. The spectra of the adhered SOA without the Teflon filter were collected. The spectra were converted to absorbance and the baseline for each spectrum was corrected using a Baseline Spline Fit (http://wavemetrics.com/project/BaselineSpline) using an Akima spline. The baseline corrected spectra were normalized to the total absorbance and smoothed with a three point rolling average to improve inter-comparison.

WM UV-Vis Spectroscopy

The remaining filter material was extracted by cutting the filter slice into small pieces and placing them in a glass vial with ~ 2 mL of acetonitrile. Samples were extracted on a shaker for ~ 2-3 h and then the liquid extract was dried under a gentle stream of ultrapure nitrogen (UHP N_2) and stored in the freezer at -20 C. Samples were reconstituted twice for subsequent analysis with UV-Vis and mass spectrometry. For UV-Vis, acetonitrile was used and, after collecting an aliquot, the solvent was again removed under gentle UHP N_2.

UV-Vis analysis was carried out using a Perkin Elmer Lambda 35 spectrometer. Each sample was reconstituted with 100 μL of acetonitrile and then 4 μL was removed and diluted with 100 μL acetonitrile in a quartz cuvette with 100 μL wells. A matching cuvette filled with acetonitrile was used as a blank. Spectra were collected from 200-800 nm with a lamp change at 324 nm and a scan speed of 450 nm min^{-1}. For MAC calculations, the concentration was estimated by assuming that 100% of the sample mass on the filter sections was extracted. If the extraction efficiency was less than 100% or if a substantial mass of material was on the small sliver removed for ATR-FTIR analysis, the MAC values here will be overestimates. The only UV-Vis data taken at WM included here is in Figure S4 panel c.

UV-Vis Data

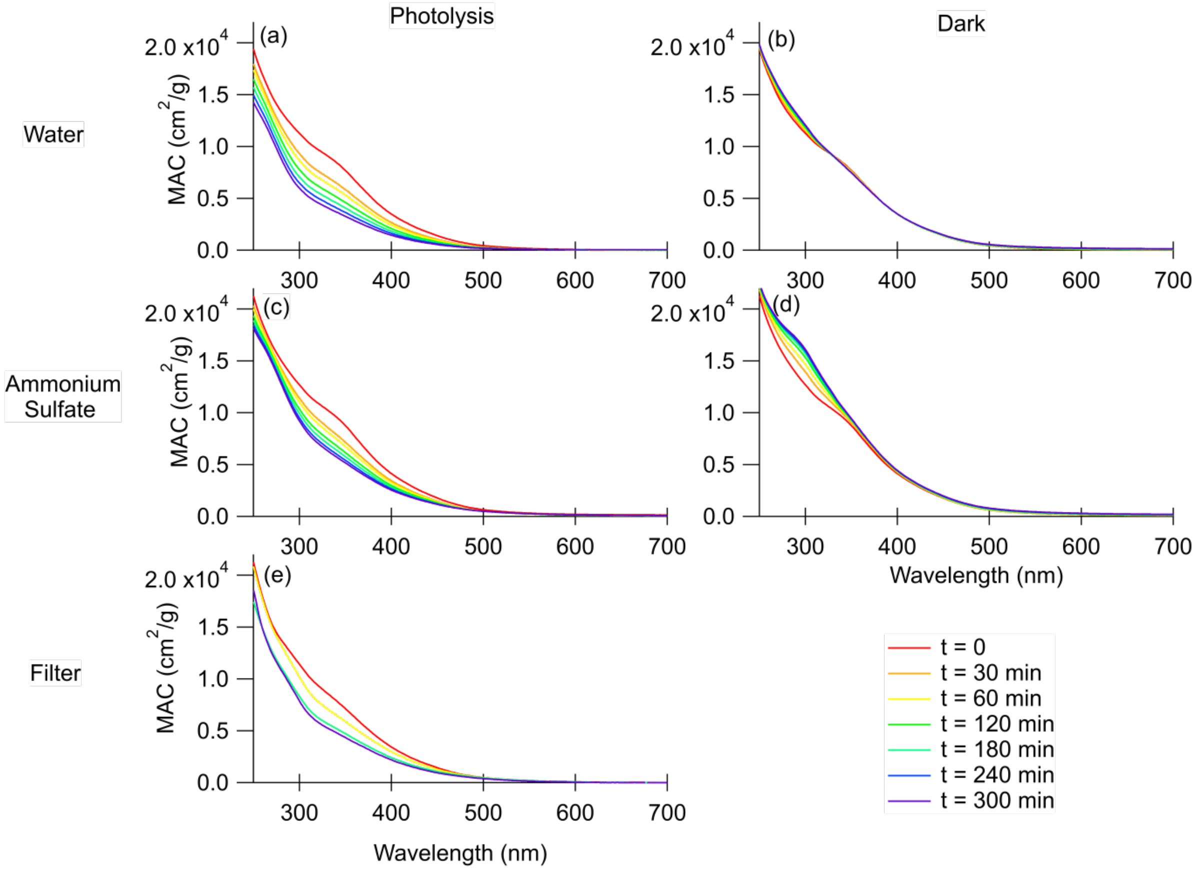

Figure S3. The wavelength-dependent mass absorption coefficient plots for each experimental condition and control. Photolysis in water is in panel (a), dark aging in water is in panel (b), photolysis in 1 M ammonium sulfate is in panel (c), dark aging in 1 M ammonium sulfate is in panel (d), and photolysis on the filter is in panel (e). Note that there are only four traces for the filter photolysis in panel e) because measuring the absorbance requires extraction of the filter and therefore is destructive.

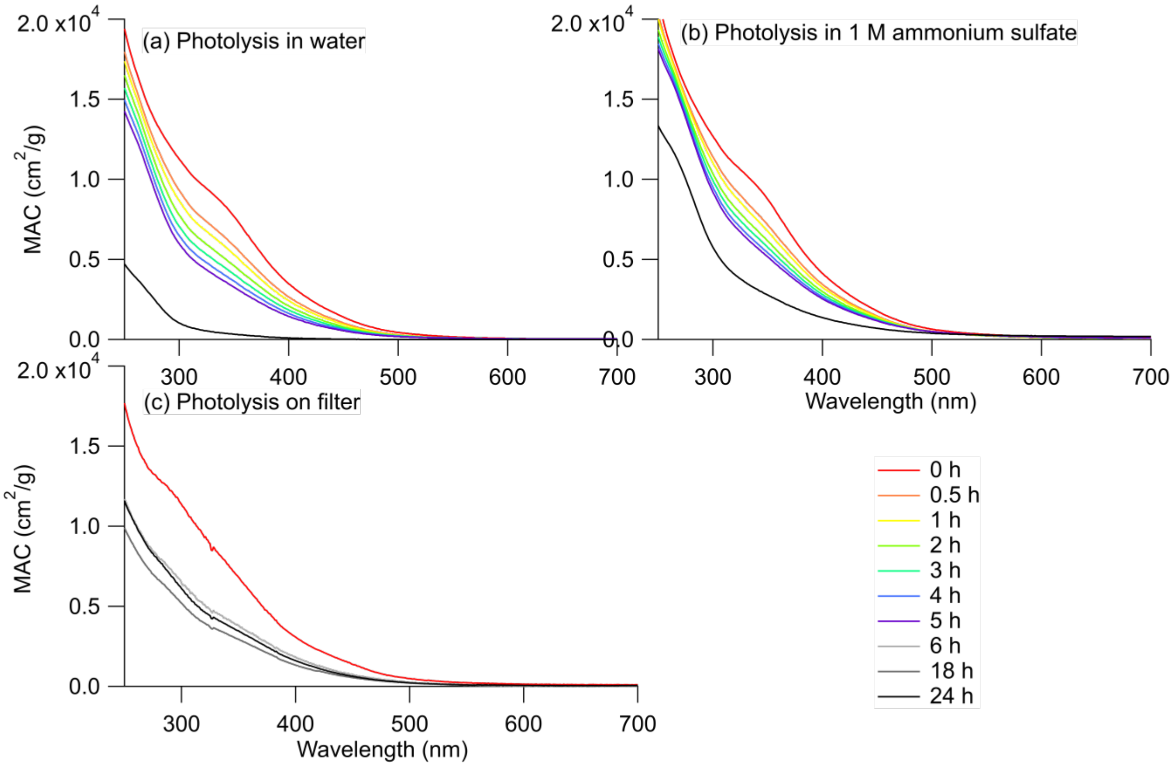

Figure S4. UV-vis absorbance spectra for toluene SOA with photolysis to 24 h. The data in panel (c) was taken at WM and photolyzed with a weaker lamp, so the time scale is not directly comparable to panels (a) and (b). However, little change is seen after 6 h of photolysis under this lamp as well.

Kinetic Measurements

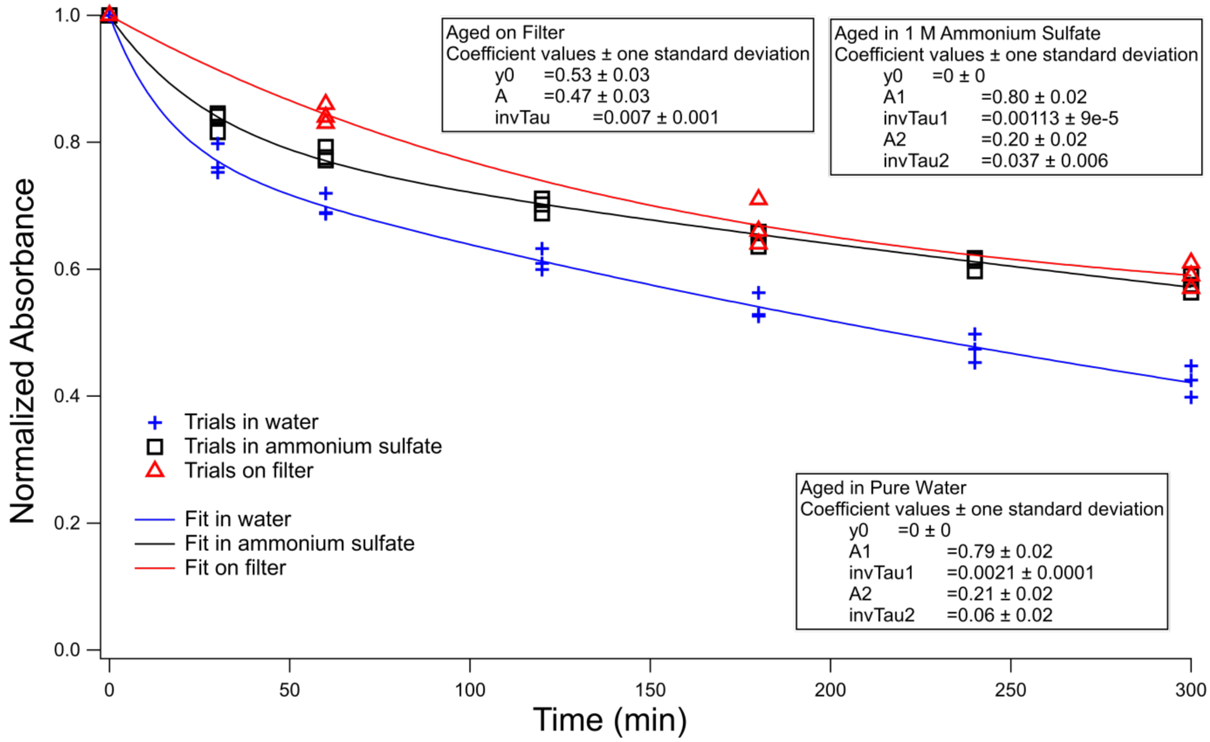

Figure S5. Rate constant fits for MAC decrease at 350 nm for each photolysis condition. Individual trials are shown with markers (water with crosses, ammonium sulfate with squares, and on the filter with triangles). Fits for the trials are shown with a solid line (blue for water, black for ammonium sulfate, and red for on the filter).

Table S4. Kinetic parameters for exponential and biexponential fits to absorbance data. Error represents the standard deviation of fitting parameters over the three combined trials.

	y_0	A_1	k_1	A_2	k_2
H_2O	0	0.79 ± 0.02	0.0021 ± 0.0001	0.21 ± 0.02	0.06 ± 0.02
AS	0	0.80 ± 0.02	0.00113 ± 0.00009	0.20 ± 0.02	0.037 ± 0.006
Filter	0.53 ± 0.03	0.47 ± 0.03	0.007 ± 0.001	NA	NA

PDA Results

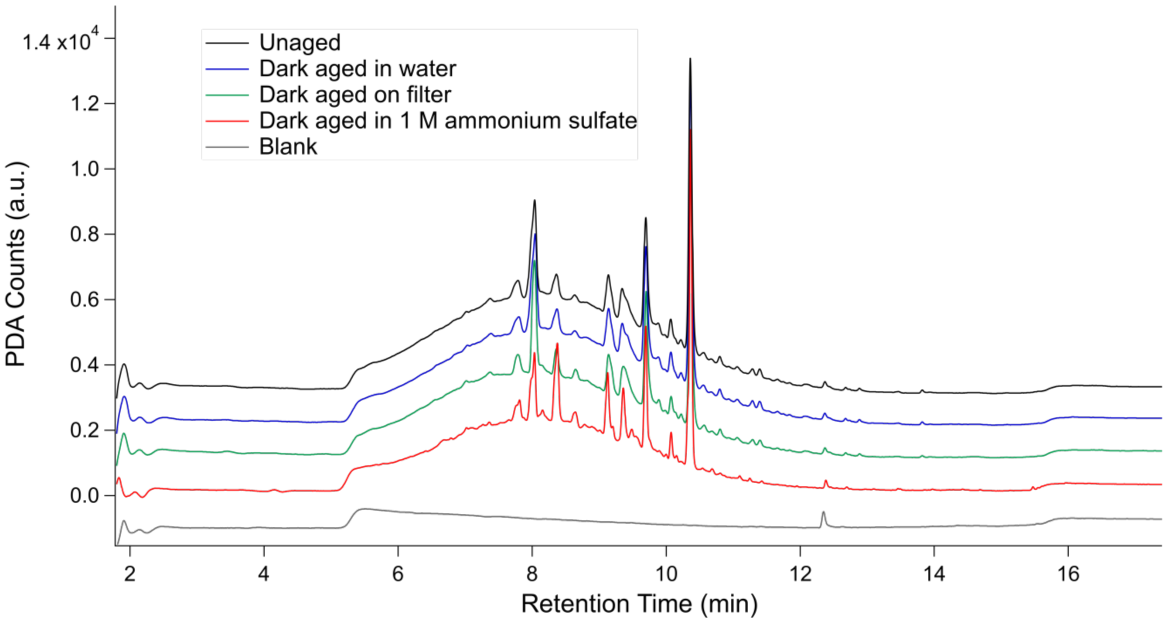

Figure S6. 2D HPLC-PDA chromatograms for all dark conditions studied. PDA counts were integrated over 340 to 360 nm wavelength range to represent the UV-Vis feature at 350 nm which decays with photolysis.

High Resolution Mass Spectrometry Results

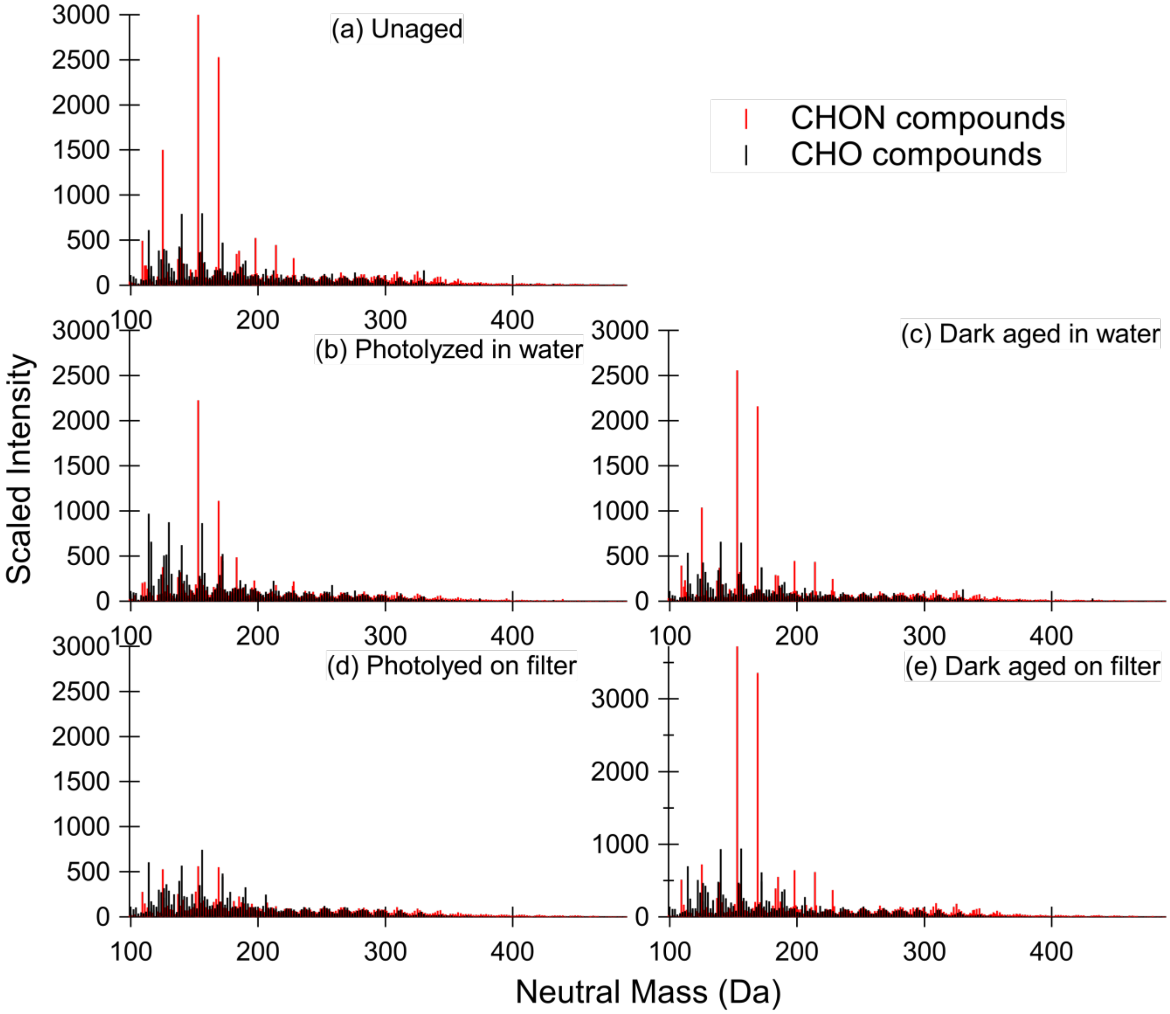

Figure S7. Mass spectra for all photolysis and dark aged samples comparing aging in water and on the filter. CHON compounds are shown in red and CHO compounds are shown in black. The three left panels are the same as in Figure 4 in the text, and the right panels show mass spectra for dark aging, which are not much different from the mass spectra for the unaged SOA.

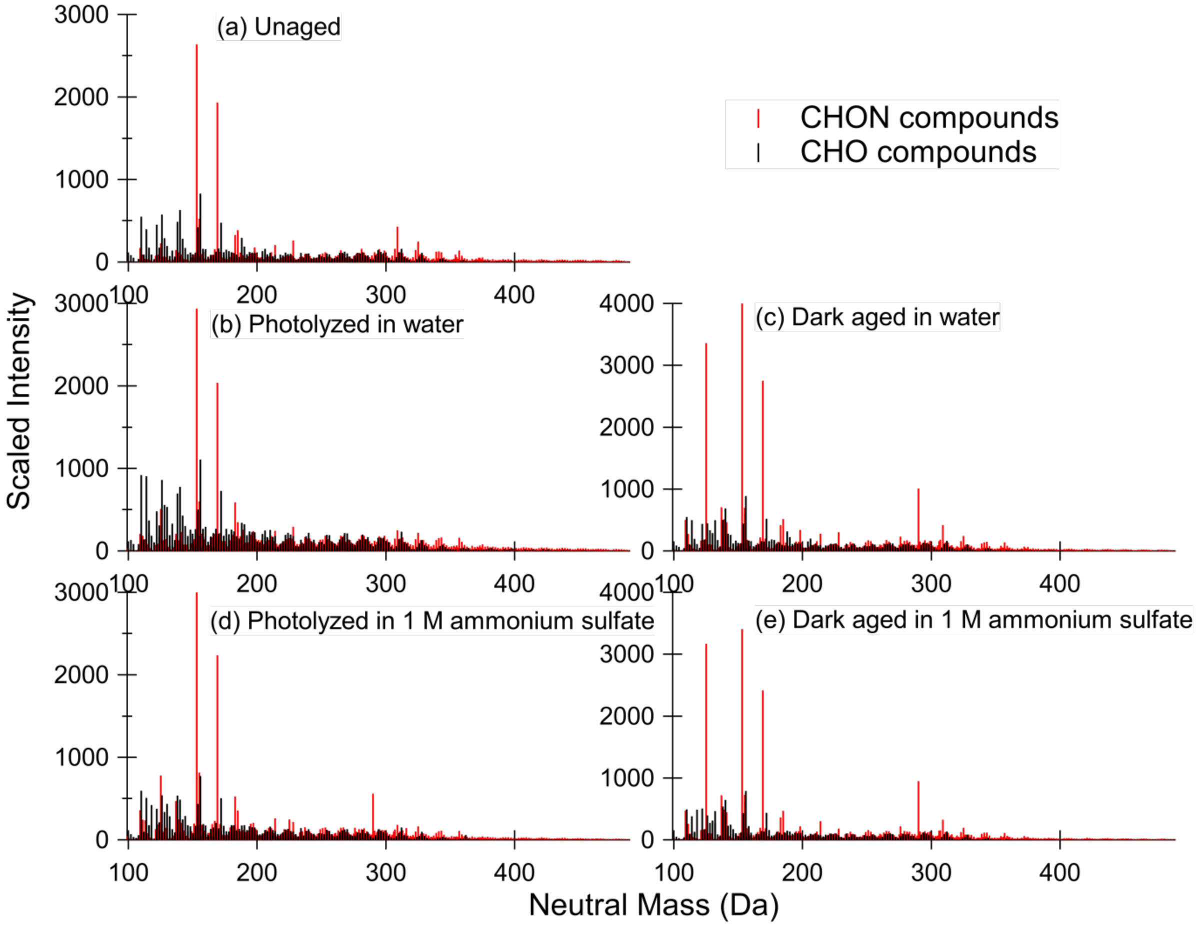

Figure S8. Mass spectra for all photolysis and dark aged samples comparing aging in water and 1 M ammonium sulfate. CHON compounds are shown in red and CHO compounds are shown in black. The three left panels are the same as in Figure 5 in the text, and the right panels show mass spectra for dark aging, which are not much different from the unaged SOA mass spectra.

ATR-FTIR Results

Figure S9 shows the evolution of the FTIR spectra of the toluene SOA during on-filter photolysis. Absorbance values are normalized to the peak intensity at 1717 cm^{-1}, which represents the carbonyl group stretching vibration. We expect carbonyl groups belonging to ketone and aldehyde functionalities to be removed through Norrish-I type reactions with photolysis (Mang et al., 2008; Lignell et al., 2013). Peaks that decrease in this plot, therefore, photolyze more readily than carbonyl compounds. Peaks corresponding to nitroaromatics (Ar-NO$_2$) and organonitrates (RONO$_2$) are denoted in the figure (Roberts, 1990; Day et al., 2010; Liu et al., 2012). It can be observed that the peaks at 1643, 1275, and 850 cm^{-1} corresponding to organonitrates decrease relative to the carbonyl peak over time. Peaks at 1556, 1539, 1360, and 1337 cm^{-1} corresponding to nitroaromatics also decrease relative to the carbonyl peak, although they do so less efficiently than the organonitrate peaks. This suggests the nitroaromatic compounds may photolyze at a slower rate than organonitrate compounds. These experiments were carried out at WM using a different lamp, so the timescales are not directly comparable with the kinetic measurements. Overall, the FTIR results show that nitrogen-containing compounds are removed during photolysis of the filters in the organic condensed phase, consistent with the HRMS results.

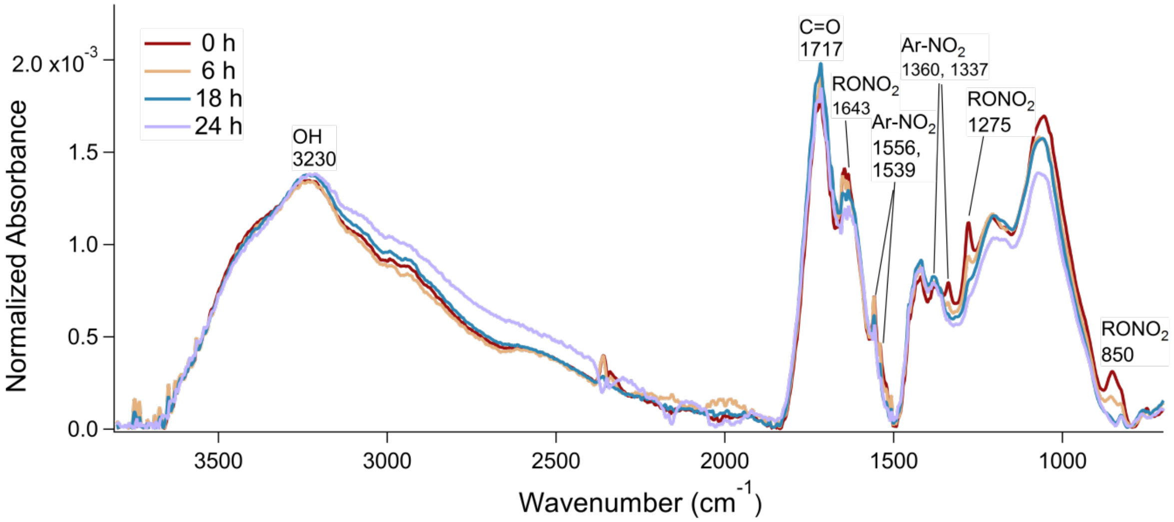

Figure S9. ATR-FTIR spectra taken after different times of on-filter photolysis normalized to the highest peak in each spectrum – the C=O peak at 1717 cm^{-1} from Filter 2. The trace for before photolysis is shown in dark red, after 6 h of photolysis in yellow, after 18 h in teal, and after 24 h in light blue. The photolysis for this experiment was performed with the irradiation set up at WM.

References

ACOM: Quick TUV: http://cprm.acom.ucar.edu/Models/TUV/Interactive_TUV/, last access: 11 July 2019.

Day, D. A., Liu, S., Russell, L. M., and Ziemann, P. J.: Organonitrate group concentrations in submicron particles with high nitrate and organic fractions in coastal southern California, Atmos. Environ., 44, 1970–1979, https://doi.org/10.1016/J.ATMOSENV.2010.02.045, 2010.

Lignell, H., Epstein, S. A., Marvin, M. R., Shemesh, D., Gerber, B., and Nizkorodov, S.: Experimental and theoretical study of aqueous cis-pinonic acid photolysis, J. Phys. Chem. A, 117, 12930–12945, https://doi.org/10.1021/jp4093018, 2013.

Liu, S., Shilling, J. E., Song, C., Hiranuma, N., Zaveri, R. A., and Russell, L. M.: Hydrolysis of organonitrate functional groups in aerosol particles, Aerosol Sci. Technol., 46, 1359–1369, https://doi.org/10.1080/02786826.2012.716175, 2012.

Mang, S. A., Henricksen, D. K., Bateman, A. P., Andersen, M. P. S., Blake, D. R., and Nizkorodov, S. A.: Contribution of carbonyl photochemistry to aging of atmospheric secondary organic aerosol, J. Phys. Chemsitry A, 8337–8344, https://doi.org/10.1021/jp804376c, 2008.

Roberts, J. M.: The atmospheric chemistry of organic nitrates, Atmos. Environ. Part A. Gen. Top., 24, 243–287, https://doi.org/10.1016/0960-1686(90)90108-Y, 1990.

Walhout, E. Q., Yu, H., Thrasher, C., Shusterman, J. M., and O'Brien, R. E.: Effects of photolysis on the chemical and optical properties of secondary organic material over extended time scales, ACS Earth Sp. Chem., 3, 1226–1236, https://doi.org/10.1021/ACSEARTHSPACECHEM.9B00109/SUPPL_FILE/SP9B00109_SI_002.TXT, 2019.